Pseudopotential-based study of gate leakage and contact resistance beyond the 10 nm node

S. Ravandi[1], Bo Fu[1], W. G. Vandenberghe[1], S. J. Aboud[2], and M. V. Fischetti[1*]
[1]Department of Materials Science and Engineering, University of Texas at Dallas, Richardson, TX 75080
[2]Energy Resources Engineering, Stanford University, Stanford CA 94305, USA
[*]e-mail: max.fischetti@utdallas.edu

ABSTRACT

Scaling FETs according to the 2011 ITRS-Roadmap and employing the empirical-pseudopotential band structure of Si and InAs thin-bodies, we show that quantum confinement causes an unacceptably large on-state gate-current leakage at gate lengths of ~5 nm. This suggests that intrinsically 2D (*e.g.*, of the graphene/graphane structure or dichalcogenides) or 1D (*e.g.*, CNTs) channels are required at 5 nm. We also report a DFT study of the metal/III-V contact resistance and present results for InAs/Mo showing that the target of 10^{-9} Ω cm^2 may be hard to achieve.

GATE LEAKAGE

The use of thinner bodies in FD-SOIs, multi-gate (MG) and nanowire (NW) FETs dictated by scaling causes an upward energy shift of the bottom of the conduction band and so an increase of the gate current (Fig. 1). Using ITRS scaling rules [1], scaling the body and insulator thickness, t_{body} and t_{ins}, linearly with gate length, L_G, adopting the EOT (0.8nm) and t_{body} (11.3nm) of the 2011 ITRS Roadmap[1] for MG-FETs at the 21 nm node, we show in Fig. 2 how the gate current, I_G, increases with decreasing gate-length. For MG-FETs I_G has been estimated in the on-state as:

$$I_G = e\int_0^{L_G} dx \quad n_s(x)\frac{\pi\hbar}{m_e t_{body}^2} T_{WKB}[\Phi_B - E_0, F_{ins}(x)]$$

where $T_{\rm WKB}[\Phi_B\text{-}E_0,F_{ins}(x)]$ is the WKB tunneling probability across the gate insulator for a barrier Φ_B reduced by the energy E_0 of the ground-state subband determined by quantum confinement (Fig. 3), $F_{ins}(x)$ is the electric field across the insulator at the position x along the channel assuming a linear source-to-drain voltage drop, and $n_s(x) = \varepsilon_{ins}F_{ins}(x)/e$ is the electron sheet density at x. The term $\pi\hbar/(m_e t_{body}^2)$ is the `attempt to escape' frequency of an electron of effective mass m_e in the ground-state subband. As seen in Fig. 2, I_G can become comparable to the on-current at short L_G. An ideal Si/HfO_2 combination appears satisfactory at ~5 nm, but the lower ε_{ins} of Al_2O_3 (resulting in physically thinner insulating layers) results in an excessively high I_G. Similarly, despite a larger semiconductor/insulator barrier, the lower InAs mass results in large quantum-confinement effects. The advantage of `intrinsically' low-dimensionality channels (of the 2D graphene /graphane structure or chalcogenides, or of the 1D CNT structure) is evident in Fig. 2 (bottom). In this case electrons are confined by the ionic potentials and the damaging effect of scaling the body thickness is avoided, in addition to allowing for thicker insulating layers. We conclude that this confinement-induced gate leakage constitutes a serious scaling limit at the 5 nm gate-length.

CONTACT RESISTIVITY

Using the DFT band-structure of Mo and InAs shown in Fig. 4, we have evaluated the InAs/Mo contact resistance [2], assuming the interface located at z=0 and conservation of parallel momentum, from:

$$\frac{1}{\rho_c} = \int_{-\infty}^{\infty} dE \frac{\partial f_S(E)}{\partial E}$$
$$\left\{ 2e^2 \sum_{n,m} \int_{\Omega_C} \frac{d\mathbf{k}}{(2\pi)^3} \upsilon_{M,n,z}(\mathbf{K},k_z) T(\mathbf{k},n,m) \delta[E - E_{M,n}(\mathbf{k})] f_M[E_{M,n}(\mathbf{k})] \right\}$$

where n and m denote the Mo and InAs bands, the integration domain Ω_c extends over 'energy-conserving' wave vectors $\boldsymbol{k}=(\boldsymbol{K},k_z)$ (*i.e.*, $E_M(\boldsymbol{K},k_z) = E_s(\boldsymbol{K},k_z')+\Phi$, where Φ is the band-discontinuity and k_z' is the normal component of the InAs wave-vector), and E_M, E_S , f_M and f_S are the dispersion and Fermi functions of Mo and InAs. Ignoring here the (all important!) overlap factor between Mo *d*-waves and InAs *sp*-waves, the 'transmitted flux' $T(\mathbf{k},n,m)$ $\upsilon_{M,n,z}(\boldsymbol{k})$ is taken as $\min[\upsilon_{M,n,z}(\boldsymbol{K},k_z), \upsilon_{S,m,z}(\boldsymbol{K},k_z')]$, the smallest of the Mo and InAs 'normal' velocity. The InAs resistance and the InAs/Mo contact resistance are shown in Fig. 4: The ITRS required 10^{-9} Ω cm^2 is at the limit of what can be practically achieved.

REFERENCES

[1] 2011 ITRS Roadmap, www.ITRS.org.. These scaling rules are very 'relaxed'. Thus, the gate current estimated here is a 'best case' scenario, but the devices do not exhibit the desired electrostatic integrity. The ITRS workgroup is at work to fix this problem (Kwok Ng, private communication).

[2] See a similar study – ignoring the effect of the metal -- by A. Baraskar *et al.*, "*High doping effects on in-situ ohmic contacts to n-InAs*", 22nd IEEE International Conference on Indium Phosphide and Related Materials, Kagawa, Japan (May 2010).

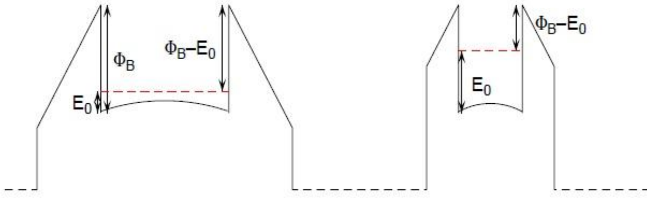

Fig. 1. Schematic diagram illustrating the reduction of the channel/insulator barrier caused by quantum confinement.

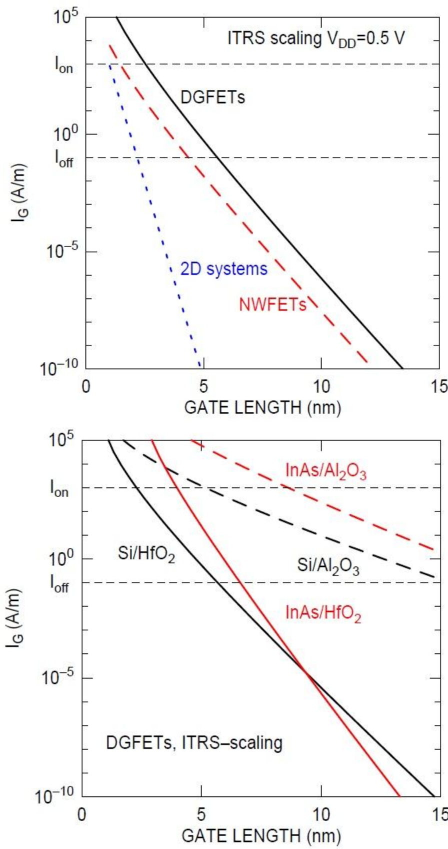

Fig. 2. *Top:* Gate current in scaled MGFETs employing a 'toy' semiconductor ($m^* = 0.25\ m_0$, nonparabolicity parameter -2.0/eV Φ_B=2.75 eV) and different device designs. '2D systems' refers to graphene (t_{body}≈0.3nm). Note their excellent behavior. *Bottom*: The same but for DG/MG-FETs only and for 'realistic' Si or InAs bodies and HfO_2 or Al_2O_3 insulators. The 2011 ITRS Roadmap scaling rules have been used in both plots.

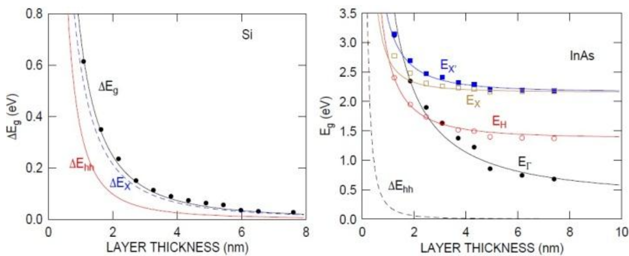

Fig. 3. Change of the gap at various 2D symmetry points for Si (H-terminated, left) and InAs (terminated by an *ad-hoc* insulator, right) thin layers *vs*. layer-thickness calculated using empirical pseudopotentials. Empirical fits to these results (lines) are employed in Fig. 2 (bottom).

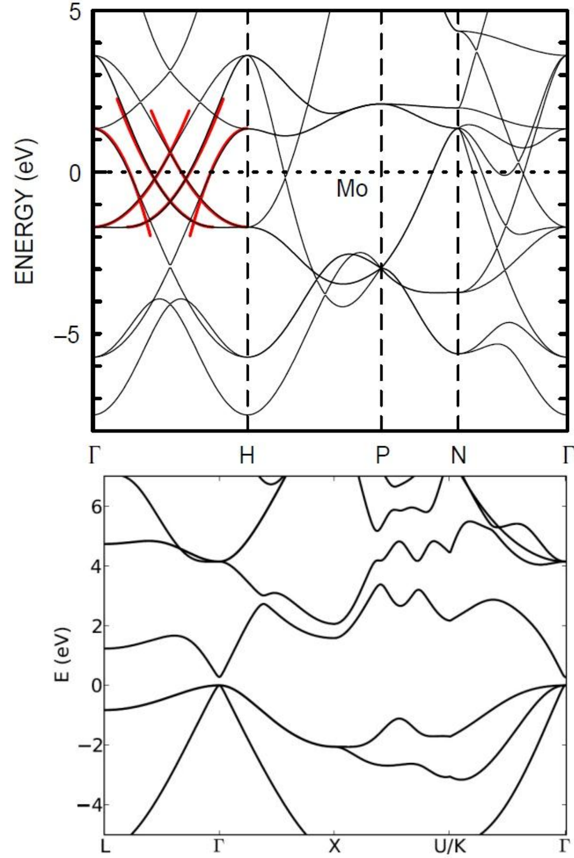

Fig. 4. DFT (Quantum Espresso) calculation of the band structure of Mo (left) and InAs (right). The thick (red) lines in the top frame show effective-mass fits to the Mo bands used to obtain the results of Fig. 5 for the (100) interface.

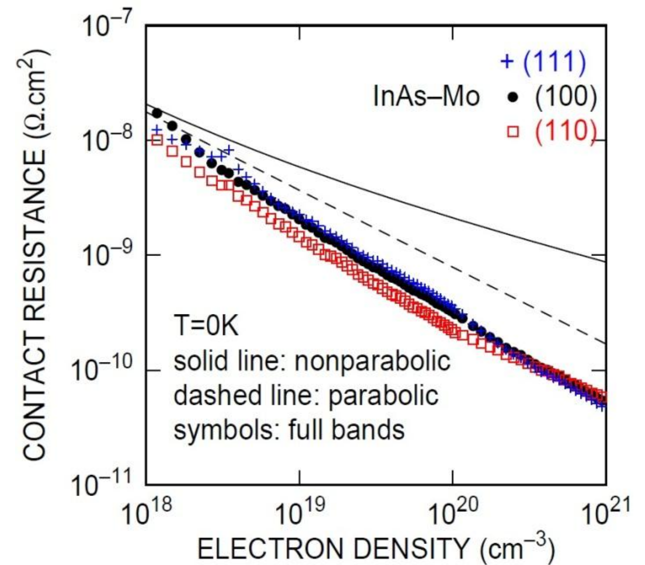

Fig. 5. Contact resistivity at the InAs/Mo interface as a function of InAs carrier density (doping). The lines show the results obtained using effective-mass models for Mo and InAs (parabolic and non-parabolic), while the symbols show results obtained using the full band structure of InAs. Since perfect wavefunction matching between the *d*-like Mo wavefunctions and the *sp*-like InAs wavefunctions has been assumed, these results should be taken as lower bounds for the contact resistivity.